Cell, Vol. 108, 371–381, February 8, 2002, Copyright ©2002 by Cell Press

A Chemical-Genetic Strategy Implicates Myosin-1c in Adaptation by Hair Cells

Jeffrey R. Holt,[1,2] Susan K.H. Gillespie,[3] D. William Provance, Jr.,[4] Kavita Shah,[5] Kevan M. Shokat,[6] David P. Corey,[1] John A. Mercer,[4] and Peter G. Gillespie[3,7,8]

[1]Massachusetts General Hospital
Harvard Medical School
Boston, Massachusetts 02114
[2]Department of Neuroscience
University of Virginia Medical School
Charlottesville, Virginia 22908
[3]Oregon Hearing Research Center
Oregon Health and Science University
Portland, Oregon 97201
[4]McLaughlin Research Institute
Great Falls, Montana 59405
[5]Genomics Institute of the Novartis Research Foundation
San Diego, California 92121
[6]Department of Cellular and Molecular Pharmacology
University of California, San Francisco
San Francisco, California 94143
[7]Vollum Institute
Oregon Health and Science University
Portland, Oregon 97201

Summary

Myosin-1c (also known as myosin-Iβ) has been proposed to mediate the slow component of adaptation by hair cells, the sensory cells of the inner ear. To test this hypothesis, we mutated tyrosine-61 of myosin-1c to glycine, conferring susceptibility to inhibition by N^6-modified ADP analogs. We expressed the mutant myosin-1c in utricular hair cells of transgenic mice, delivered an ADP analog through a whole-cell recording pipette, and found that the analog rapidly blocked adaptation to positive and negative deflections in transgenic cells but not in wild-type cells. The speed and specificity of inhibition suggests that myosin-1c participates in adaptation in hair cells.

Introduction

Hair cells, the sensory cells of the inner ear, transduce auditory and vestibular stimuli into receptor potentials, which initiate transmission of the sensory signal to the central nervous system. Mechanical transduction is carried out by the hair bundle, a crosslinked cluster of ~50 actin-filled stereocilia arranged in ranks of increasing height. This anatomical polarity corresponds to the physiological polarity of the bundle, so that deflections of the bundle toward the tallest stereocilia depolarize the cell, deflections toward the shortest stereocilia hyperpolarize the cell, and perpendicular deflections have no effect on the membrane potential. Hair-cell transduction is direct: bundle deflections stretch ~50 gating springs, which tug open 50–100 cation-selective transduction channels within microseconds and without second-messenger intervention (Corey and Hudspeth, 1983). Although transduction channels open and close stochastically, changes in gating-spring tension alter the channels' open probability (P_{open}) and change the total receptor current flowing through them.

Hair cells adapt to sustained bundle deflections by adjusting the open probability of transduction channels back toward a resting level, a process which can be assessed either by observing the decay of receptor current or by measuring the instantaneous relationship between deflection and current (the I(X) curve). Adaptation occurs in two phases (reviewed in Eatock, 2000). Fast adaptation, complete within a few milliseconds, occurs when Ca^{2+} enters open transduction channels and binds to a site on or near the channels; when Ca^{2+} binds, channels close (Howard and Hudspeth, 1988; Crawford et al., 1991). By contrast, slow adaptation, which takes place over tens of milliseconds, is thought to be carried out by adaptation motors (Howard and Hudspeth, 1987; Assad and Corey, 1992; Gillespie and Corey, 1997; Holt and Corey, 2000). The motors are hypothesized to link transduction channels to the actin core of the stereocilium, climbing along the stereocilium to adjust the resting tension on the channels. In response to the increased tension applied by an excitatory stimulus (and to Ca^{2+} entering through opened transduction channels), the motor slips, gating-spring tension decreases, and channels close. The adaptation motor may also play an essential role in assembling and properly biasing the transduction apparatus of hair cells in all organs of the inner ear.

Four lines of circumstantial evidence implicate myosin molecules in slow adaptation. First, slow adaptation is not merely a passive response to the stimulus; the adaptation motor actively generates force (Assad and Corey, 1992). Second, slow adaptation takes place within actin-rich stereocilia (Flock et al., 1981), and myosins are the only motor molecules known to move along actin. Third, slow adaptation requires Ca^{2+} and calmodulin (Walker and Hudspeth, 1996), both of which control the activity of unconventional myosins. Fourth, ADP analogs and phosphate analogs, inhibitors of myosin activity, block slow adaptation (Gillespie and Hudspeth, 1993; Yamoah and Gillespie, 1996). Candidates for the adaptation motor are therefore likely to belong to the extensive myosin superfamily (Berg et al., 2001).

Although several myosin isozymes are present in hair bundles (Gillespie et al., 1993; Hasson et al., 1997), the best supported adaptation-motor candidate is myosin-1c (Myo1c), previously named myosin-Iβ (Sherr et al., 1993) and myr 2 (Ruppert et al., 1995). Myo1c is present in bundles in sufficient quantity to carry out adaptation (Gillespie et al., 1993; Walker and Hudspeth, 1996) and is located near stereociliary tips (Gillespie et al., 1993; Hasson et al., 1997), where transduction and adaptation take place. Electron-microscopic immunolocalization places Myo1c at the submembranous anchors of tip links (Garcia et al., 1998; Steyger et al., 1998), the extracellular

[8]Correspondence: gillespp@ohsu.edu

filaments thought either to be the gating springs or to connect in series with them (Kachar et al., 2000). Localization data necessarily fall short, however, of demonstrating that Myo1c actually mediates adaptation.

To test the hypothesis that Myo1c participates in adaptation, we have applied a chemical-genetic strategy for selectively inhibiting its motor activity. We designed a mutation in Myo1c, Y61G, that greatly increased its sensitivity to inhibition by N^6-modified ADP analogs (Gillespie et al., 1999). This scheme is based on similar strategies for modifying other nucleoside triphosphatases, such as conversion of GTPases to XTPases (Rybin et al., 1996), and modification of protein kinases to permit them to use N^6-modified ATP analogs (Shah et al., 1997) or to be inhibited by pyrazolo-pyrimidine-based inhibitors (Bishop et al., 2000b). Because the adaptation-motor complex likely consists of dozens of myosin molecules working together (Gillespie and Corey, 1997), immobilization of only a fraction of these molecules in an actin-bound state should be required to arrest adaptation. We therefore made transgenic mice that express Y61G-Myo1c, and found that slow adaptation is blocked when hair cells are dialyzed with N^6(2-methyl butyl) ADP (NMB-ADP).

Results

Inhibitor–Sensitized Mutant Strategy

To allow selective Myo1c inhibition, we sought to create a mutation that would have little effect on ATP hydrolysis and motor activity, but would sensitize the myosin to an inhibitor that we could supply to hair cells. Tyrosine-135 of myosin II forms a hydrogen bond with the N^6-amino group of ADP (Fisher et al., 1995; Figure 1A). When we mutated the homologous tyrosine residue in Myo1c (Y61) to glycine, the resulting Y61G-Myo1c hydrolyzed ATP with velocity and kinetics similar to those of wild-type Myo1c (Gillespie et al., 1999). The Y61G substitution expanded the nucleotide binding pocket, permitting N^6-modified nucleotide analogs such as NMB-ADP (Figure 1B) to bind to Y61G-Myo1c much more tightly than to wild-type. An ADP analog is the most appropriate inhibitor, since it should cause myosin to remain tightly bound to actin in a rigor-like state (Cooke and Pate, 1985; Gillespie and Hudspeth, 1993). NMB-ADP was an effective and selective inhibitor of Y61G-Myo1c. The combination of mutant Myo1c and NMB-ADP produced a dominant effect on in vitro motility in mixtures of wild-type and mutant Myo1c; only a small fraction of Y61G-Myo1c was required for robust inhibition by the ADP analog (Gillespie et al., 1999).

Efficient adaptation presumably requires ATP-hydrolytic activity of all myosins in the adaptation-motor complex (Figure 1D and Gillespie and Corey, 1997). In a mixed complex, immobilization of mutant myosins by NMB-ADP should halt movement of the entire complex (Figure 1E). We created a theoretical model (P.G.G., unpublished) for transduction and adaptation in wild-type or Y61G-expressing hair cells that combines an adaptation-motor formalism (Shepherd and Corey, 1994) with adaptation-motor properties inferred from in vitro assays (Gillespie et al., 1999). The model predicted that NMB-ADP should inhibit adaptation in hair cells when Y61G-Myo1c makes up as few as 10% of the total Myo1c molecules (Figures 1F and 1G, and data not shown).

Y61G Is Expressed in Hair Cells of Transgenic Mice

To apply this inhibitor-sensitization strategy to hair cells, we generated transgenic mice that expressed Y61G-Myo1c. We sought to ensure that the levels and cellular distribution of Y61G-Myo1c expression were similar to those of endogenous, wild-type Myo1c. To do so, we fused ~6 kbp of mouse *Myo1c* 5′ genomic DNA, including the first coding exon and part of the second, to a cDNA encoding rat Myo1c (Figure 2A). Although this construct did not include a native distal transcription start site (Pestic-Dragovich et al., 2000), we nevertheless expected that the ~4 kbp of genomic DNA upstream of the proximal transcription start site would be sufficient to drive transgenic expression. We analyzed two founder lines (Y61G-33 and Y61G-36) with the Y61G mutation; a third transgenic line (wt-42), in which the transgene encoded the wild-type mouse-rat chimeric Myo1c, was generated for control experiments.

Although RT-PCR experiments detected steady-state levels of message expressed by the transgene, the intron between the first and second coding exons was inefficiently spliced out (not shown). Because this unspliced intron encoded 35 amino acids, in frame with the remainder of the transgene, the intron-containing mRNA might encode a functional protein. To circumvent any problems that might be caused by the expression of this alternative protein, we made a second transgenic construct that lacked this intron (Figure 2A). In one founder line examined in detail, Y61G-9018, mRNA transcribed from the transgene accounted for ~30% of the total Myo1c transcript population in the lung and ~65% in the utricle (Figure 2B).

To confirm expression of Y61G-Myo1c in transgenic hair cells, we purified hair bundles (Figure 2C) from wild-type and transgenic mice. Using a sensitive pan-Myo1c antibody and standardizing to the amount of bundle actin, we found that bundles from Y61G-9018 transgenic mice had ~35% more Myo1c than did bundles from wild-type mice (Figure 2D). In addition, bundles from Y61G-33 transgenic mice had ~65% more total Myo1c than bundles from wild-type littermates (data not shown). Since each wild-type mouse stereocilium contains fewer than 200 molecules of Myo1c (Dumont et al., 2002), the immunoblot data suggest that stereocilia of Y61G-9018 transgenic mice also contain fewer than 200 molecules of Y61G-Myo1c. Unfortunately, the scarcity of Myo1c prevented us from selectively detecting Y61G-Myo1c in bundles of transgenic hair cells using anti-epitope tag antibodies (not shown).

No Consequences of Y61G-Myo1c Expression in the Absence of NMB-ADP

We used whole-cell, tight-seal recording and mechanical stimulation of wild-type and transgenic hair cells to determine whether mutant Myo1c interfered with adaptation. Adaptation in mouse utricular hair cells is dominated by relatively slow adaptation (Holt et al., 1997). Dialyzing utricular hair cells with a whole-cell recording pipette, we simultaneously deflected hair bundles with

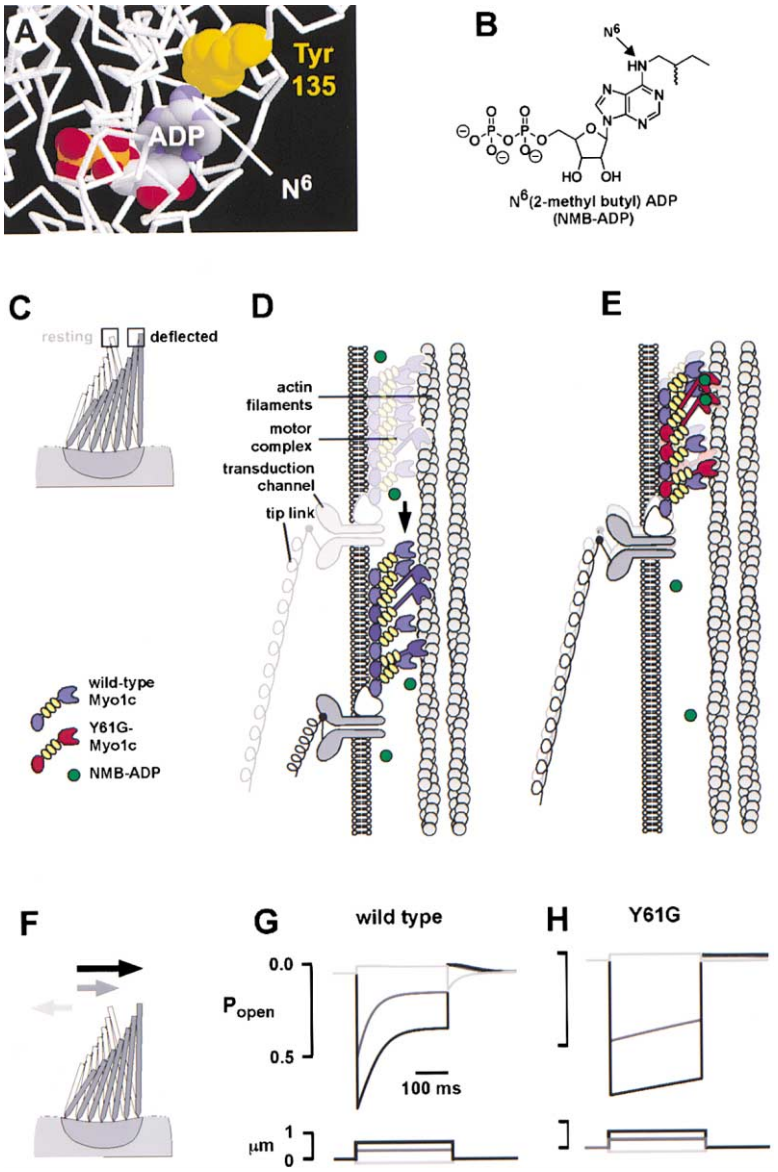

Figure 1. Inhibitor-Sensitization Strategy and Predicted Effects of NMB-ADP on Adaptation

(A) Structure of the nucleotide binding site of *Dictyostelium discoideum* myosin II with bound ADP (CPK colors); note the proximity of Tyr-135 (yellow) to the N^6 position of ADP. Figure drawn with RasMol using the PDB file 1MND.

(B) NMB-ADP structure; N^6 nitrogen is indicated.

(C) Hair bundle undergoing a positive step deflection; light and dark colors indicate before and after step.

(D) Model for adaptation of wild-type transduction apparatus to positive deflection. A cluster of Myo1c molecules, making up the adaptation-motor complex ("motor complex"), anchors the transduction channel and associated proteins to the actin filaments of the stereociliary core. Positive deflections increase tension on all elements; Myo1c molecules, unable to resist tension as they traverse through the weak binding states of their ATPase cycles, slip down the cytoskeleton and permit adaptation. NMB-ADP (green circles), which does not bind at low concentrations to wild-type Myo1c, is not expected to affect wild-type adaptation.

(E) Expected block of adaptation in Y61G hair cells by NMB-ADP. When Y61G-Myo1c molecules (red) are incorporated in the adaptation-motor complex and NMB-ADP molecules lock them in a rigor-like state, the tension produced by positive deflections can no longer move the motor complex. Sustained deflections produce sustained tension and transduction channels remain open.

(F) Hair bundle undergoing step deflections (not to scale); arrows indicate relative size and polarity of stimuli modeled in (G) and (H).

(G) Predicted lack of effect of 250 μM NMB-ADP on adaptation in wild-type hair cells. Model responses to –0.3, +0.3, and +0.6 μm stimuli.

(H) Predicted block of adaptation by 250 μM NMB-ADP in hair cells expressing 50% Y61G-Myo1c, 50% wild-type Myo1c.

a fluid jet or with a stiff probe and recorded transduction currents. As noted previously (Holt et al., 1997), fluid-jet and stiff-probe stimulation did not yield identical adaptation properties and hence were analyzed separately. To rule out the possibility that our results were caused by insertion of the transgene into a specific genomic location, we examined transduction and adaptation in detail in three independent mouse lines expressing Y61G-Myo1c (Y61G-33, Y61G-36, and Y61G-9018). To demonstrate that inhibitor effects with these mouse lines resulted from expression of the Y61G mutant transgene, we also analyzed transduction and adaptation in a control wild-type transgenic line (wt-42).

Because Y61G-Myo1c behaved similarly to wild-type in the presence of ATP in vitro, its expression should have few effects on hair cell properties in the absence of the inhibitor. Indeed, transduction and adaptation in hair cells from the Y61G-33 and Y61G-36 lines in the absence of NMB-ADP were very similar to those in wild-type cells (Figures 3B and 3C). In seven wild-type and eight transgenic hair cells examined in detail, current-deflection (I(X)) plots were very similar (Figures 3D and 3E), with similar maximal transduction currents (~200 pA) and similar parameter values from fits of a second-order Boltzmann model. In the absence of stimulation, the resting open probability of the transduction channels in the hair cells expressing Y61G-Myo1c (0.034 ± 0.008) was higher than that for wild-type hair cells (0.017 ± 0.007) when measured using a protocol that avoids artifacts from stimulator-induced mechanical bias (see Experimental Procedures). For positive deflections that initially opened about half of the channels, time constants for adaptation were similar for wild-type (τ = 42 ± 9 ms) and Y61G (τ = 50 ± 7 ms) littermates. The rate of adaptation to negative steps, a consequence of how quickly the adaptation-motor complex climbs up the side of a stereocilium, was unchanged in hair cells expressing Y61G-Myo1c (0.36 ± 0.07 μm s^{-1}, expressed as the

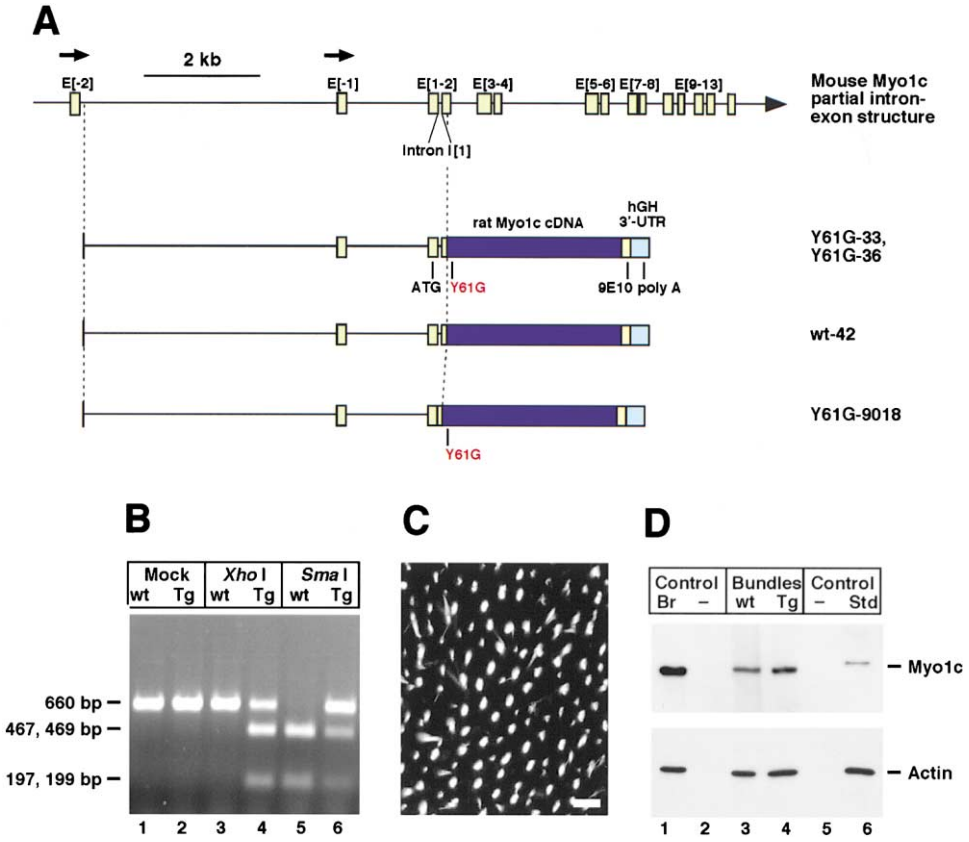

Figure 2. Expression of Y61G-Myo1c in Transgenic Mice

(A) Genomic interval and transgenic constructs. Top, intron-exon structure of the 5′ end of the mouse *Myo1c* locus (Hamilton et al., 1997); exons E[−1] and E[−2] contain alternative transcription start sites (Pestic-Dragovich et al., 2000). Bottom, a cDNA encoding rat Myo1c was fused to the middle of the second coding exon of mouse Myo1c. One construct incorporated the Y61G mutation; a second control construct used the wild-type rat sequence. A third construct, with the Y61G mutation, deleted intron I[1].

(B) RT-PCR analysis of spliced mRNA in Y61G-9018 mouse utricles. RT-PCR was carried out on utricular cDNA using primers that amplify both wild-type and transgenic cDNA. Restriction-endonuclease treatment was used to estimate the relative amounts of wild-type and transgenic cDNA; XhoI only cuts transgenic cDNA (lanes 3 and 4) and SmaI only cuts wild-type cDNA (lanes 5 and 6).

(C) Isolated mouse hair bundles, imbedded in agarose and stained with rhodamine-phalloidin.

(D) Immunoblot detection of Myo1c in wild-type and Y61G-9018 transgenic hair bundles. Approximately 20 utricular equivalents of bundles (from 40 utricles) were loaded on each lane. Br, 2 μg of mouse brain extract. Std, 50 pg of Myo1c or 50 ng of human platelet actin (85% β-actin, 15% γ-actin). Negative control (–), equivalent amount of agarose without bundles.

motor velocity along actin filaments; wild-type controls, 0.32 ± 0.06 μm s^{-1}). Although they were not statistically significant, these small effects of Y61G-Myo1c expression on properties of transduction and adaptation in the absence of NMB-ADP are consistent with our predictions of the effect of increased Myo1c levels in transgenic bundles.

No Effect of NMB-ADP on Wild-Type or Wild-Type-Transgenic Hair Cells

To confirm that NMB-ADP did not interfere with transduction in hair cells, we examined transduction and adaptation in wild-type littermates of Y61G mice and in transgenic mice expressing a wild-type transgene. When hair cells from these mice were dialyzed with 100 or 250 μM NMB-ADP, no effects on adaptation were seen (Figures 4B and 4C), even after protracted dialysis of >30 min.

Four hair cells from nontransgenic littermates, dialyzed with 250 μM NMB-ADP and stimulated with stiff probes, were analyzed in detail. Adaptation properties from hair cells of these FVB × C57BL/6 F_1 hybrid mice (Figure 5) were consistent with those from outbred CD-1 mice (Figure 4A and Holt et al., 1997). For example, the time constant for adaptation to a positive step that opened half the channels in these four cells (51 ± 9 ms) was indistinguishable from that for nine CD-1 hair cells (49 ± 6 ms). Likewise, adaptation properties of 15 wild-type hair cells, dialyzed with 100 or 250 μM NMB-ADP and stimulated with a fluid jet, were similar to those of CD-1 mice with fluid-jet stimulation (Holt et al., 1997, and data not shown).

To test adaptation under these control conditions more thoroughly, we applied an adapting step to a hair bundle, then used short test deflections to examine the effect of the adapting step on the I(X) curve. Because the adaptation motor modulates the position of the I(X) curve, a shift of the curve should reflect the movement of the motor (Eatock et al., 1987). Figures 6A and 6B show families of currents evoked by this protocol, recorded ~20 min following breakthrough to whole-cell

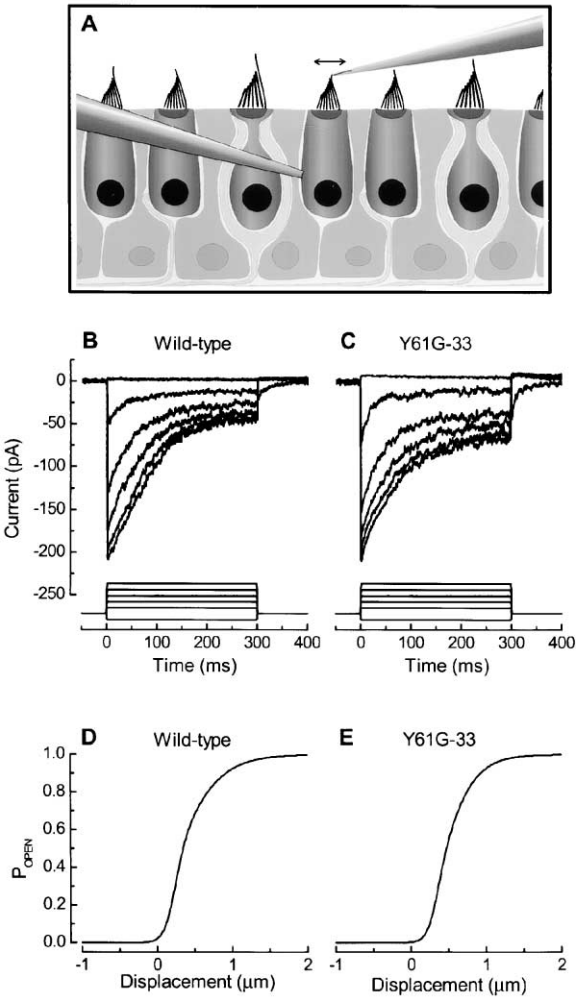

Figure 3. Similarity of Transduction Currents in Wild-Type and Transgenic Hair Cells in the Absence of NMB-ADP

(A) Schematic diagram illustrating the recording configuration. The recording pipette (left) contained the standard intracellular solution with or without NMB-ADP, depending on the experiment. The stimulus pipette (right) was tightly coupled to the hair bundle. In this image, deflections to the right open channels and are defined as positive.

(B) Transduction currents from wild-type hair cell in response to 300 ms deflections of −0.5 μm to 1.5 μm.

(C) Transduction currents from a hair cell of a Y61G-33 transgenic mouse.

(D) Average I(X) relation generated from seven wild-type hair cells. Individual curves were fit with a second-order Boltzmann equation; fit parameters were averaged and transduction currents were expressed as open probability.

(E) Average I(X) relation generated from eight Y61G-33 hair cells.

mode in a wt-42 transgenic hair cell. Prolonged dialysis with 250 μM NMB-ADP did not affect how quickly and how far the I(X) curve shifted in response to positive or negative deflections (Figures 6C and 6D).

Finally, we analyzed adaptation in Y61G transgenic hair cells with NMB-ADP in the recording pipette before the nucleotide had time to diffuse to the stereocilia (Figures 4E–4H, thin traces). We observed robust transduction and adaptation in most hair cells, indistinguishable from recordings from other Y61G cells in the absence of the nucleotide analog.

NMB-ADP Blocks Adaptation When Y61G-Myo1c Is Present

In contrast to the normal adaptation observed in control conditions, adaptation in Y61G hair cells was blocked within a few minutes when the ADP analog was delivered through a whole-cell pipette (Figures 4E–4H). A delay of a few minutes is consistent with the time required for diffusion of the analog into the cell; with the series resistances of our dialysis pipettes, the time constant for NMB-ADP analog entry into hair cells should be 2–4 min (Pusch and Neher, 1988). Diffusion from the soma to stereociliary tips should lengthen this delay. Adaptation was blocked in hair cells from mice from all 3 mutant transgenic lines (Figures 4E–4H). Similar results were seen with fluid-jet stimulation, although fewer cells lost adaptation completely (not shown).

As whole-cell dialysis proceeded, the fraction of Y61G-Myo1c-expressing hair cells that retained any adaptation to positive deflections fell to ~50% (Figure 5A). In those cells that retained adaptation, the adaptation rate constant ($1/\tau$) fell from 19 ± 1 s^{-1} to 8 ± 1 s^{-1}. Furthermore, the extent of adaptation fell from an initial value of 68% ± 2% to only 32% ± 9%, which would be predicted with progressive immobilization of individual adaptation-motor complexes. The initial rate of adaptation, the product of these values, was 5-fold slower in Y61G-Myo1c hair cells than in wild-type cells (Figure 5B).

The block of adaptation to positive and negative deflections also was reflected in the shifts of I(X) curves during adapting steps, which were rapidly inhibited by NMB-ADP in hair cells expressing Y61G-Myo1c (Figures 6E–6H). In addition, I(X) relations broadened during inhibition of adaptation; in Y61G-expressing cells, the deflection required to increase P_{open} from 0.1 to 0.9 expanded from an initial value of 0.78 ± 0.10 μm to 1.49 ± 0.30 μm (n = 5) after NMB-ADP dialysis (e.g., Figures 6E–6H).

We noticed several unexpected phenomena in Y61G hair cells as NMB-ADP blocked adaptation. First, as the nucleotide exerted its effects, amplitudes fell by 30%–60% within a few minutes (Figures 4E–4H). By contrast, transduction currents of wild-type hair cells with NMB-ADP or Y61G hair cells without the analog typically remained stable over ten or more minutes (Figures 4A–4D). Second, when a hair bundle was returned to its rest position after a positive deflection, channel closing slowed noticeably (asterisks in Figures 4E–4G). Double-exponential fits of channel closure yielded time constants of 3–4 ms and 10–20 ms for the fast and slow components.

Large negative deflections are thought to remove external forces from adaptation motors and permit them to climb along the actin cytoskeleton at a constant rate (Assad and Corey, 1992). When the hair bundle is returned to its rest position, large overshoot currents appear that result from the amount of negative adaptation that ensued during the prior negative deflection (Figure 7A). Adaptation to negative deflections was particularly sensitive to NMB-ADP in hair cells expressing Y61G-Myo1c; the current overshoots disappeared over the course of the experiment

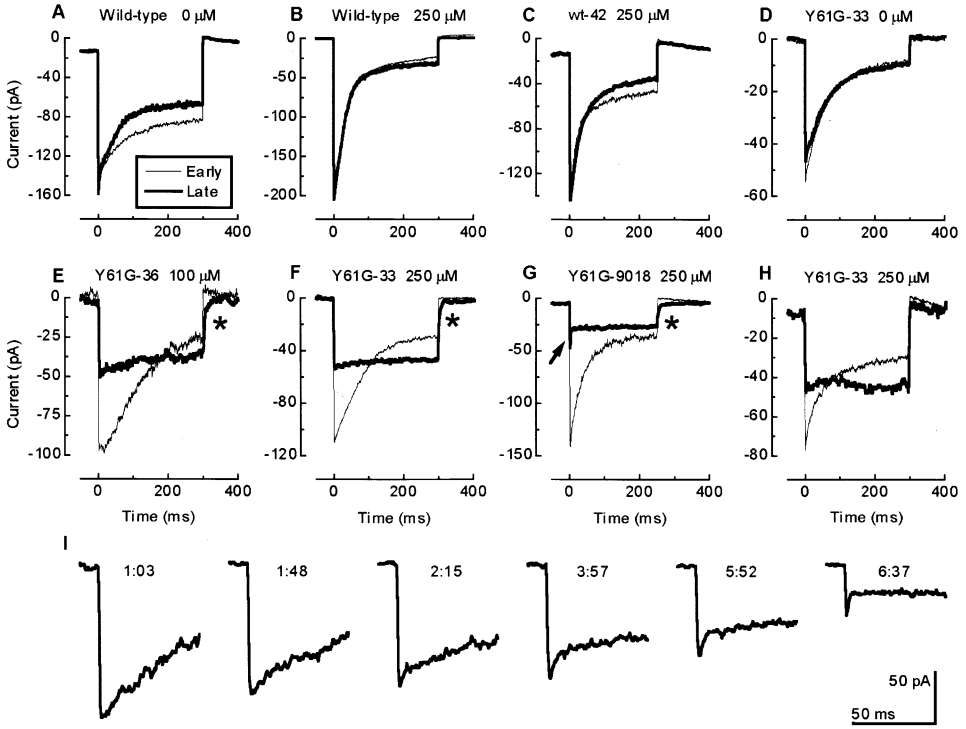

Figure 4. Adaptation to Positive Deflections for Wild-Type and Transgenic Hair Cells Before and After Dialysis with the Pipette Solution

(A) Wild-type hair cell without NMB-ADP. Traces at 4 and 12 min; 0.6 μm deflections. Note fast phase of adaptation.

(B) Wild-type hair cell with 250 μM NMB-ADP. Traces at 6 and 21 min; 1.0 μm deflections.

(C) wt-42 (wild-type transgenic) hair cell with 250 μM NMB-ADP. Traces at 4 and 22 min; 0.5 μm deflections.

(D) Y61G-33 hair cell without nucleotide analog. Traces at 2 and 17 min; 0.8 μm deflections.

(E) Y61G-36 hair cell with 100 μM NMB-ADP. Traces at 4 and 7 min; 0.6 μm deflections. Asterisk indicates slow closing kinetics; a double-exponential fit gave time constants of 2.6 and 10.4 ms.

(F) Y61G-33 hair cell with 250 μM NMB-ADP. Traces at 1 and 4 min; 0.6 μm deflections. Asterisk, channel-closure time constants of 3.6 and 18.7 ms.

(G) Y61G-9018 hair cell with 250 μM NMB-ADP. Traces at 1 and 4 min; 0.8 μm deflections. Arrow, fast adaptation appearing after slow adaptation is blocked. Asterisk, channel-closure time constants of 3.8 and 36 ms.

(H) Y61G-33 hair cell with 250 μM NMB-ADP. Traces at 1 and 5 min; 0.3 μm deflections.

(I) Progression of slow-adaptation block for cell shown in (G). Time after whole-cell configuration was established are indicated.

(Figure 7B), indicating that adaptation was completely blocked. Nearly all cells expressing the Y61G transgene that initially displayed negative adaptation in response to stiff-probe stimulation eventually lost adaptation (Figure 5C). By contrast, loss of negative adaptation was never seen in wild-type hair cells dialyzed with NMB-ADP and stimulated by a stiff probe (Figure 5C) or a fluid jet (data not shown).

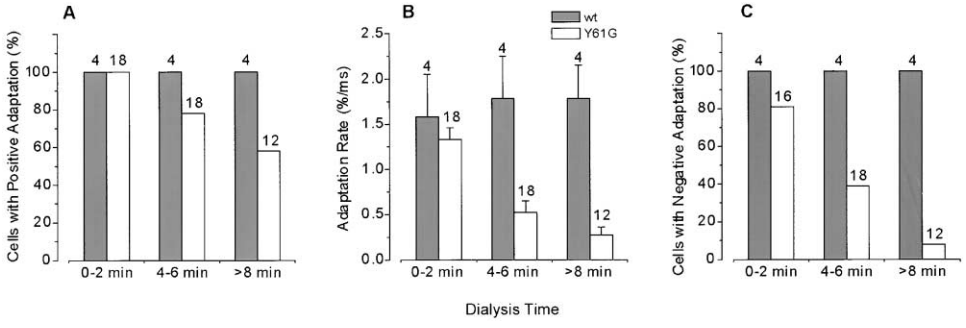

Figure 5. Summary of Adaptation Properties for Y61G-33 and Wild-Type Hair Cells Dialyzed with 250 μM NMB-ADP

Data were collected from wild-type and Y61G hair cells using stiff-probe stimulation. All cells analyzed had minimum transduction currents of 50 pA and were held for at least 6 min.

(A) Cells with positive adaptation.

(B) Initial adaptation rate expressed as percent change per millisecond of the initial current evoked by the deflection. Error bars indicate SEM.

(C) Cells with negative adaptation remaining at indicated times. For each panel, number of cells analyzed is indicated above bars.

Block of adaptation by NMB-ADP in Y61G-9018 hair cells was qualitatively similar, although the fraction of cells not showing adaptation at the beginning of the recording was surprisingly high (7/14). With one exception, hair cells that did adapt initially lost adaptation to both positive and negative deflections if the recording continued for at least 8 min (e.g., Figure 4G).

Because the proposed mechanisms for fast (<5 ms) and slow (>10 ms) adaptation are fundamentally distinct (Howard and Hudspeth, 1988; Crawford et al., 1991), fast adaptation may persist when slow adaptation is blocked. Although fast adaptation was rarely apparent in utricle hair cells under control conditions, in 4 out of 18 Y61G-33 hair cells and 2 out of 14 Y61G-9018 hair cells, NMB-ADP simultaneously blocked slow adaptation and revealed a residual fast component (Figures 4G and 4I). The time constant for the fast decay of current was 4.9 ± 1.3 ms, similar to that seen in hair cells from bullfrog (Benser et al., 1996; E. Cheung and D.P.C., unpublished) and somewhat slower than that in turtle (Wu et al., 1999). The fast decay was only seen during a positive deflection and remained for the duration of the recording in most cells.

Discussion

Using a method that combines genetics and chemistry, we have demonstrated that hair cell Myo1c participates in adaptation of mechanoelectrical transduction. Determining the function of a specific molecule in a complex biological system taxes modern methods of analysis. Targeted gene deletion, although powerful, only tests the first essential role for a molecule, which could favor developmental phenotypes that mask later physiological roles. In addition, redundancy can mask important functions of the deleted gene. Cell- or stage-specific conditional knockouts can circumvent some of these problems, but the phenotype can still depend on the speed of protein degradation. Dominant-negative overexpression experiments can be informative, but depend on features of each individual system and are often nonselective.

Introduction of a mutation to permit inhibition by an otherwise inactive ligand largely circumvents problems associated with gene targeting (Bishop et al., 2000a). By designing an otherwise silent mutation that sensitized Myo1c to N^6-modified nucleotides, and by introducing the inhibitory nucleotide within a few minutes during continuous observation, we avoided the problems associated with other approaches. Conveniently, mutant Myo1c behaved almost normally in the absence of NMB-ADP and was expressed at lower levels than wild-type Myo1c. Even if Myo1c plays a critical role in hair-cell or hair-bundle formation, the presence of functional Myo1c molecules ensured that hair cells developed normally prior to electrophysiological recording. Furthermore, we could acutely inhibit the mutant Myo1c within a few minutes, likely preventing compensation by the cell. Because adaptation was rapidly inhibited in hair cells expressing Y61G-Myo1c only when NMB-ADP was supplied, Myo1c must participate in adaptation.

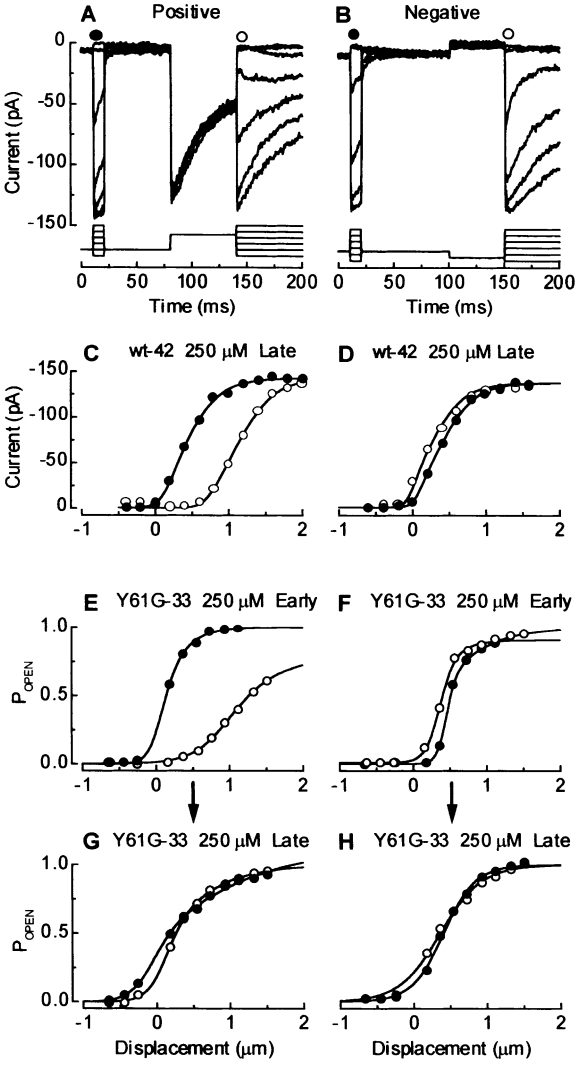

Figure 6. Inhibition of Adaptive Shift of I(X) Relation

(A) Transduction currents (top) in response to a stimulus protocol (bottom) for measuring adaptation to positive deflections, recorded from a wt-42 transgenic hair cell dialyzed for 20 min with 250 μM NMB-ADP.

(B) Currents and protocol for analysis of adaptation to negative deflections of the same hair cell.

(C) Adaptive shift of current-displacement relation from the data in (A). Filled circles indicate the I(X) relation evoked from the rest position; hollow circles indicate the adapted I(X) relation. Both curves were fit with a second-order Boltzmann relation.

(D) Adaptive shift for a negative deflection derived from the data in (B).

(E) Adaptive shift for positive deflection of Y61G-33 hair cell, 18 min after initiating dialysis with 250 μM NMB-ADP. Note large (normal) shift.

(F) Adaptive shift for negative deflection of Y61G-33 hair cell, 18 min after initiating dialysis with 250 μM NMB-ADP. As in control cells, the shift was modest.

(G) Adaptive shift for positive deflection for the cell in (E), 22 min after dialysis began. The shift was completely blocked.

(H) Adaptive shift for negative deflection for the cell in (F), 22 min after dialysis began. Shift was completely blocked. Note that the inhibitory effects of NMB-ADP were slow to develop in this particular cell; the "early" time points of (E) and (F) are later than early time points of Figure 4.

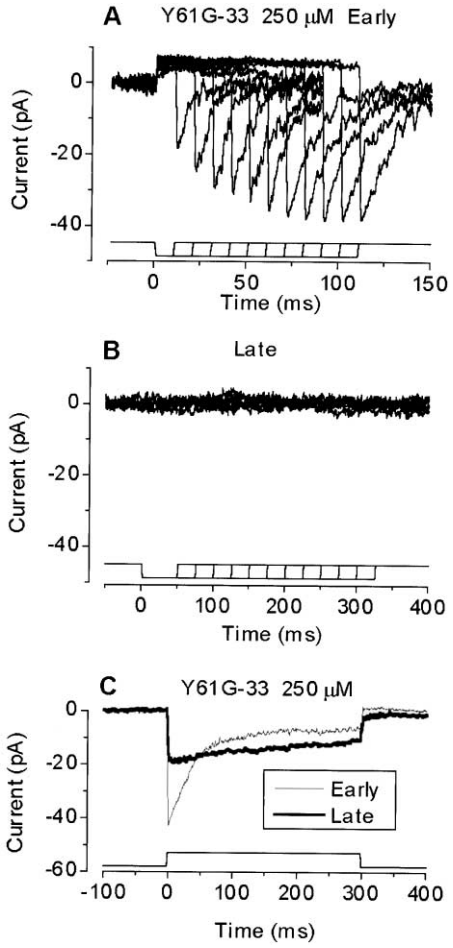

Figure 7. Rebound Currents after Negative Steps

(A) Top, adaptation to –0.8 μm inhibitory displacements of varying duration in a Y61G hair cell 3 min after initiating dialysis with NMB-ADP. The stimulus protocol is indicated at the bottom. Note increasing rebound currents with increased step duration, reflecting an increased amount of negative adaptation with time.

(B) Same cell, 21 min into dialysis; all rebound currents have disappeared.

(C) Transduction in response to positive deflections (0.8 μm) was not abolished, although the rate of adaptation and extent of adaptation decreased.

A Chemical-Genetic Strategy to Probe Protein Function

The specific inhibitor-sensitization strategy used here (Gillespie et al., 1999) has advantages and disadvantages over similar approaches. Conversion of kinesins to accept N^6-modified ATP analogs (Kapoor and Mitchison, 1999) and mutations of GTPases to accept xanthine triphosphate (Rybin et al., 1996) eliminated activity of the modified enzymes with the native nucleotide. By contrast, our mutant retained nearly normal enzymatic utilization of ATP, as in the strategies employed for protein kinases (Shah et al., 1997; Bishop et al., 2000a). Because the motor presumably requires ATP-dependent motility to move it to the site of adaptation, inactivation of Myo1c's native ATPase activity would be undesirable in our experiments. On the other hand, the choice of a modified nucleotide for the inhibitor has some drawbacks. N^6-modified ADP analogs are negatively charged and must be introduced into cells by whole-cell dialysis, microinjection, or cell permeabilization. Cells also may convert the diphosphate analogs into triphosphates, changing their physiological effects. We circumvented these drawbacks here by studying one cell at a time; we could easily set the cytoplasmic nucleotide concentration and avoid metabolic conversion by dialysis with the recording electrode. We also presumably avoided adenylate kinase conversion of the analog (Gillespie and Hudspeth, 1993) by including a high concentration of ATP in the pipette, which should inhibit binding of NMB-ADP molecules to adenylate kinase (Shioda et al., 1991).

Mutant Myo1c Participates in Slow Adaptation

Because the adaptation-motor complex is thought to contain dozens of myosin molecules, insertion of Y61G-Myo1c into the complex should sensitize adaptation to NMB-ADP. Indeed, NMB-ADP largely blocked the hair cell's ability to adapt to mechanical stimuli in transgenic mice expressing Y61G-Myo1c. The effects of NMB-ADP were not due to overexpression of the mutant myosin for two reasons: first, overall expression levels were low, relative to wild-type Myo1c; second, adaptation in transgenic mice expressing a wild-type version of the transgene was entirely normal, even with NMB-ADP present. Because the biochemical properties of Y61G-Myo1c are otherwise very similar to those of the wild-type myosin (Gillespie et al., 1999), we conclude that Myo1c must be part of the adaptation-motor complex.

An alternative interpretation remains possible: perhaps Y61G-Myo1c does not actively participate in adaptation, but instead resides along the actin tracks of the adaptation-motor complex. NMB-ADP would immobilize these myosin molecules, blocking movement of the complex, as do high concentrations of N-ethylmaleimide-modified myosin-II (Cande, 1986). This alternative explanation is highly unlikely, due to the system's geometry and the low ratio of Y61G-Myo1c to actin in a stereocilium. We found that adaptation to deflections as small as 300 nm was completely blocked by NMB-ADP (Figure 4H). Because of the bundle's geometry and incomplete extent of adaptation (Holt et al., 1997), adaptation to such a step under control conditions requires an average motor movement of ~8 nm, hardly more than the diameter of a single actin monomer. For adaptation to both positive and negative deflections to be blocked in transgenic hair cells with deflections of this size, at least one of the fewer than 200 Y61G-Myo1c molecules in a stereocilium must have bound to at least one actin filament both immediately above and immediately below the adaptation motor. Because the outer surface of the stereociliary actin bundle comprises ~70,000 actin monomers, chance disposition next to the adaptation motor of rare Y61G-Myo1c molecules—simultaneously in all ~50 stereocilia—is improbable. Moreover, if they are not components of the motor, these blocking myosins would not be mechanically coupled to the adaptation motor; the motor might just step around them. Instead, the most likely explanation is that Myo1c is an integral part of the adaptation motor and participates in adaptation.

We were surprised by two features of the block of adaptation by NMB-ADP in Y61G hair cells. First, transduction

current amplitudes usually fell by ~30%–60% (Figures 4E–4H). This effect is reminiscent of a similar effect of calmodulin inhibitors (Walker and Hudspeth, 1996); current amplitudes may have decreased because of complete loss of some of the ~50 individual transduction units in a hair cell. Normally, the adaptation mechanism should protect transduction from protracted mechanical stimuli like those we applied. A second surprising result after inhibition was that channels closed more slowly when bundles were returned to their rest position. Turtle hair cells exhibited a similar reduction of channel closing rate during dialysis with BAPTA, upon depolarization, or as extracellular Ca^{2+} was reduced (Crawford et al., 1991), all of which block adaptation. Inhibition of slow adaptation therefore affects properties of the transduction channel, perhaps indirectly.

Our present data are confined to the neonatal mouse vestibular system, so it remains possible that other myosin isozymes mediate adaptation in mature vestibular hair cells or in auditory hair cells. In addition, Myo1c inhibition should prevent motility of other functionally coupled motor proteins, so we cannot yet conclude that Myo1c is the only myosin isozyme of the adaptation-motor complex. For example, myosin-VIIa has been proposed to anchor transduction channels in cochlear hair cells, generating force and acting like the adaptation motor (Kros et al., 2002). Application of this chemical-genetic approach to mature vestibular hair cells, to auditory hair cells, and to other myosin isozymes known to be important for hair cells, such as myosin-VIIa, can address these points.

Separation of Fast and Slow Adaptation

In a striking separation of slow and fast adaptation (Wu et al., 1999; Holt and Corey, 2000; Eatock, 2000), we sometimes observed a fast phase of current decay that persisted even when the slow phase was abolished by NMB-ADP. Although fast adaptation was not observed in all NMB-ADP-treated cells, such adaptation was difficult to observe in control cells; moreover, fast adaptation is most pronounced for stimuli smaller than we usually delivered. Because fast adaptation acts as a high-pass filter and utricular hair cells are optimized for detection of low-frequency stimuli (Holt et al., 1999), utricular hair cells may not universally exploit this mechanism. Even though not all utricular hair cells show fast adaptation, we expect to be able to use Y61G-expressing hair cells to independently investigate Ca^{2+} and second-messenger control of fast and slow adaptation.

Conclusions

The demonstration that Myo1c participates in adaptation shows that this motor is a component of the hair cell transduction complex, and should assist identification of additional components of the complex. Our experiments also provide one of the very few demonstrations of the role of an unconventional myosin in a metazoan cell. Finally, the chemical-genetic strategy described here will be useful for defining functions of Myo1c in other cell types, functions of other myosin isozymes in multiple cell types, and—with appropriate modification—functions of other essential molecules in complex biological systems.

Experimental Procedures

Myosin Nomenclature

Several different names are used in the literature for Myo1c, including myosin-Iβ and myr 2 (Berg et al., 2001). In agreement with the myosin-I field (Gillespie et al., 2001), we use here the name adopted by the Human Genome Organization (HUGO; http://www.gene.ucl.ac.uk/nomenclature/). Myo1c is the abbreviation for myosin-1c, the protein product of the mouse gene *Myo1c*.

Myo1c Transgenic Constructs

We identified a 150 kbp clone from a genomic 129/Sv mouse bacterial artificial chromosome library (Genome Systems) and subcloned into pZERO2.1 a 13 kbp BamHI fragment. This subclone starts at nucleotide 64,835 of GenBank accession number U96726 (Hamilton et al., 1997) and continues beyond the end of that sequence. We subcloned from that a 6.5 kbp KpnI fragment into pGEM-7Z and added by mutagenesis an AgeI site at nucleotides 5907–5912. An AgeI-SpeI fragment of Y61G rat Myo1c, including a C-terminal c-*myc* epitope and the human growth hormone 3′UTR and polyadenylation signal (Gillespie et al., 1999), was ligated to the genomic Kpn fragment in pGEM-7Z, previously cut with AgeI and SpeI. A Kpn-Spe fragment of the resulting construct was injected into fertilized FVB/N oocytes, which were implanted into recipient pseudopregnant mice. Progeny of two founders, Y61G-33 and Y61G-36, were analyzed. We also made a construct that was identical except that it lacked the Y61G mutation, generating the wild-type transgenic line wt-42. Finally, we generated a construct with the Y61G mutation in which we precisely deleted the intron between coding exons 1 and 2; the progeny of one founder, Y61G-9018, were analyzed. Transgenic and wild-type mice were identified by PCR.

RT-PCR Analysis of Transgenic mRNA Expression

We purified total RNA (RNeasy, Qiagen) from utricles of genotyped mice, synthesized cDNA using oligo(dT)-containing primers, and carried out PCR (ThermoScript RT-PCR, Gibco-BRL). To ensure that we only analyzed spliced mRNA, we carried out RT-PCR using a forward primer (5′-CGGTTCCGGGAGAACCTCATTTATAC-3′) that spans exons 1 and 2. The reverse primer (5′-AGCGCCTTCCTCA CAACCTTCCAGTC-3′) was 100% complementary to rat Myo1c sequence present in the transgenic construct; mouse Myo1c differs by only a single nucleotide in position 14. To estimate the relative fraction of wild-type and transgenic mRNA, we treated the PCR products with the restriction endonucleases XhoI, which only cuts rat (transgenic) cDNA, or with SmaI, which only cuts mouse (wild-type) cDNA. Ethidium bromide-stained gels were quantified using an imaging system (Alpha Innotech, San Leandro, CA).

Analysis of Transgenic Protein Expression

We isolated hair bundles by adapting the twist-off method (Gillespie and Hudspeth, 1991) to neonatal mouse utricles (Dumont et al., 2002). After sticking dissected utricles to a chamber with Cell-Tak (BD Biosciences), we manually removed their otolithic membranes, imbedded the utricles in 4% low-melting-point agarose, and sheared their bundles off. Recoveries of 50% were typical. Proteins in bundles pooled from wild-type or transgenic mice were separated by SDS-PAGE, transferred to a PVDF blotting membrane. Myo1c was detected by immunoblotting with 5 μg/ml R2652 antibody, which recognizes the C-terminal 15 kDa of mouse and rat Myo1c (Dumont et al., 2002); blots were developed with an HRP-conjugated secondary antibody and an HRP substrate that produces a chemiluminescent product (SuperSignal West Pico, Pierce, Rockford, IL). After stripping the blot, we detected bundle actin using the N350 anti-actin antibody (Amersham-Pharmacia Biotech). Myo1c and actin were quantified by densitometry of film images, using for calibration known amounts of purified proteins, which were also included on the immunoblots.

Electrophysiology

For all electrophysiological experiments, we used F_1 hybrids of FVB/N hemizygous transgenic male and C57BL/6 wild-type female mice. We carried out physiology experiments on wild-type and transgenic littermates, insuring that the expressed transgene was the only difference in genetic background. We genotyped mice before or after electrophysiological experiments by PCR.

Sensory epithelia of utricles were excised from neonatal mice as previously described (Holt et al., 1997); we observed similar results with utricles harvested from postnatal day 1 to 8 mice. The utricle dissection was performed in standard external solution, which contained (in mM) 144 NaCl, 0.7 NaH_2PO_4, 5.8 KCl, 1.3 $CaCl_2$, 0.9 $MgCl_2$, 5.6 D-glucose, and 10 HEPES-NaOH; the solution was adjusted to pH 7.4 and 320 mmol kg^{-1} osmolality. To remove the otolithic membrane, the tissue was bathed for 20 min in 100 μg/ml type XXVII protease (Sigma, St. Louis, MO) dissolved in standard external solution. The sensory epithelium was mounted in an experimental chamber on a fixed-stage upright microscope (Axioskop FS; Zeiss, Oberkochen, Germany) and viewed with a 63$\times$ water-immersion objective with differential interference contrast optics.

The experimental chamber contained standard extracellular solution. Recording pipettes contained standard intracellular solution, which included (in mM): 140 KCl, 0.1 $CaCl_2$, 5 EGTA-KOH, 3.5 $MgCl_2$, 2.5 MgATP, and 5 HEPES-KOH; pH 7.4 and 290 mmol kg^{-1}. NMB-ADP was synthesized as described (Gillespie et al., 1999) and added to standard internal solution at 100 or 250 μM. Recording electrodes were pulled with resistances of 3–5 MΩ from R-6 soda lime glass (Garner Glass, Claremont, CA), and had series resistance of 8–12 MΩ when sealed to cells. We recorded from hair cells in the intact epithelium using the whole-cell, tight-seal technique (Hamill et al., 1981) and an Axopatch 200B patch-clamp amplifier (Axon Instruments, Foster City CA). Cells were held at -60 mV; transduction currents were filtered at 2 kHz with an 8-pole Bessel filter (Model 902, Frequency Devices, Haverhill, MA), digitized at $\geq$4 kHz using a 12-bit acquisition board (Digidata 1200) and pClamp 8.0 software (both from Axon Instruments), and recorded on hard disk. Analysis and fits were done with Origin 6.0 (Microcal Software, Northampton, MA). Results are presented as means $\pm$ standard error of the mean.

For some experiments, hair bundles were deflected using a fluid jet, controlled by a fast pressure-clamp system (Holt et al., 1997). For other experiments, bundles were deflected using a stiff glass pipette (Figure 3A). The distal portion of the kinocilium was drawn into a glass pipette of tip diameter $<$1 μm; the bundle was tightly coupled to the pipette by applying a constant negative pressure at the back end. The pipette was mounted on a piezoelectric bimorph that had submillisecond rise times in response to square command steps supplied by the Digidata 1200.

To measure adaptation parameters, records from stimuli that elicited a P_{open} of $\sim$0.5 were fit with double exponentials. Although adaptation rate is most accurately measured with a multiple-pulse step protocol (Eatock et al., 1987), confining analysis to these stimuli ensured that currents remained in the near-linear region of the I(X) relation. The inverse of the time constant for the slower component was taken as the adaptation rate constant and the extent of adaptation was calculated by dividing the extrapolated steady-state transduction current by the peak transduction current. Resting P_{open} was determined in some cells by measuring total membrane current prior to attaching the stimulator and by subsequently measuring current for saturating positive and negative deflections. From the original resting current, P_{open} could be calculated without influences from the static bias applied by the stimulator.

Acknowledgments

We thank Donna Klinedinst (Johns Hopkins University) for assembly of the original transgenic construct, Dee Goss (McLaughlin Research Institute) for oocyte injections, Colleen Silan (McLaughlin Research Institute) for genotyping, and Kevin Nusser (Oregon Health and Science University) for hair-bundle isolation and genotyping. This work was supported by NIH grants DC03279 (J.A.M., P.G.G., and J.R.H.), CA70331 (K.M.S.), DC00304 (D.P.C.), and DC02368 (P.G.G.). D.W.P. was supported by the Oberkotter Foundation and D.P.C. is an investigator with the Howard Hughes Medical Institute.

Received August 14, 2001; revised January 3, 2002.

References

Assad, J.A., and Corey, D.P. (1992). An active motor model for adaptation by vertebrate hair cells. J. Neurosci. *12*, 3291–3309.

Benser, M.E., Marquis, R.E., and Hudspeth, A.J. (1996). Rapid, active hair bundle movements in hair cells from the bullfrog's sacculus. J. Neurosci. *16*, 5629–5643.

Berg, J.S., Powell, B.C., and Cheney, R.E. (2001). A millennial myosin census. Mol. Biol. Cell *12*, 780–794.

Bishop, A., Buzko, O., Heyeck-Dumas, S., Jung, I., Kraybill, B., Liu, Y., Shah, K., Ulrich, S., Witucki, L., Yang, F., et al. (2000a). Unnatural ligands for engineered proteins: new tools for chemical genetics. Annu. Rev. Biophys. Biomol. Struct. *29*, 577–606.

Bishop, A.C., Ubersax, J.A., Petsch, D.T., Matheos, D.P., Gray, N.S., Blethrow, J., Shimizu, E., Tsien, J.Z., Schultz, P.G., Rose, M.D., et al. (2000b). A chemical switch for inhibitor-sensitive alleles of any protein kinase. Nature *407*, 395–401.

Cande, W.Z. (1986). Preparation of N-ethylmaleimide-modified heavy meromyosin and its use as a functional probe of actomyosin-based motility. Methods Enzymol. *134*, 473–477.

Cooke, R., and Pate, E. (1985). The effects of ADP and phosphate on the contraction of muscle fibers. Biophys. J. *48*, 789–798.

Corey, D.P., and Hudspeth, A.J. (1983). Kinetics of the receptor current in bullfrog saccular hair cells. J. Neurosci. *3*, 962–976.

Crawford, A.C., Evans, M.G., and Fettiplace, R. (1991). The actions of calcium on the mechano-electrical transducer current of turtle hair cells. J. Physiol. (Lond.) *434*, 369–398.

Dumont et al. (2002). Myosin-I isozymes in neonatal rodent auditory and vestibular epithelia. J. Assoc. Res. Otolaryngol. *3*, in press.

Eatock, R.A. (2000). Adaptation in hair cells. Annu. Rev. Neurosci. *23*, 285–314.

Eatock, R.A., Corey, D.P., and Hudspeth, A.J. (1987). Adaptation of mechanoelectrical transduction in hair cells of the bullfrog's sacculus. J. Neurosci. *7*, 2821–2836.

Fisher, A.J., Smith, C.A., Thoden, J.B., Smith, R., Sutoh, K., Holden, H.M., and Rayment, I. (1995). X-ray structures of the myosin motor domain of *Dictyostelium discoideum* complexed with MgADP•BeF_x and MgADP•AlF_4^-. Biochemistry *34*, 8960–8972.

Flock, A., Cheung, H.C., Flock, B., and Utter, G. (1981). Three sets of actin filaments in sensory cells of the inner ear. Identification and functional orientation determined by gel electrophoresis, immunofluorescence, and electron microscopy. J. Neurocytol. *10*, 133–147.

Garcia, J.A., Yee, A.G., Gillespie, P.G., and Corey, D.P. (1998). Localization of myosin-Iβ near both ends of tip links in frog saccular hair cells. J. Neurosci. *18*, 8637–8647.

Gillespie, P.G., and Corey, D.P. (1997). Myosin and adaptation by hair cells. Neuron *19*, 955–958.

Gillespie, P.G., and Hudspeth, A.J. (1991). High-purity isolation of bullfrog hair bundles and subcellular and topological localization of constituent proteins. J. Cell Biol. *112*, 625–640.

Gillespie, P.G., and Hudspeth, A.J. (1993). Adenine nucleoside diphosphates block adaptation of mechanoelectrical transduction in hair cells. Proc. Natl. Acad. Sci. USA *90*, 2710–2714.

Gillespie, P.G., Wagner, M.C., and Hudspeth, A.J. (1993). Identification of a 120 kd hair-bundle myosin located near stereociliary tips. Neuron *11*, 581–594.

Gillespie, P.G., Gillespie, S.K., Mercer, J.A., Shah, K., and Shokat, K.M. (1999). Engineering of the myosin-Iβ nucleotide-binding pocket to create selective sensitivity to N^6-modified ADP analogs. J. Biol. Chem. *274*, 31373–31381.

Gillespie, P.G., Albanesi, J.P., Bähler, M., Bement, W.M., Berg, J.S., Burgess, D.R., Burnside, B., Cheney, R.E., Corey, D.P., Coudrier, E., et al. (2001). Myosin-I nomenclature. J. Cell Biol. *155*, 703–704.

Hamill, O.P., Marty, A., Neher, E., Sakmann, B., and Sigworth, F.J. (1981). Improved patch-clamp techniques for high-resolution current recording from cells and cell-free membrane patches. Pflugers Arch. *391*, 85–100.

Hamilton, B.A., Smith, D.J., Mueller, K.L., Kerrebrock, A.W., Bronson,

R.T., van Berkel, V., Daly, M.J., Kruglyak, L., Reeve, M.P., Nemhauser, J.L., et al. (1997). The vibrator mutation causes neurodegeneration via reduced expression of PITP α: positional complementation cloning and extragenic suppression. Neuron *18*, 711–722.

Hasson, T., Gillespie, P.G., Garcia, J.A., MacDonald, R.B., Zhao, Y., Yee, A.G., and Corey, D.P. (1997). Unconventional myosins in inner-ear sensory epithelia. J. Cell Biol. *137*, 1287–1307.

Holt, J.R., and Corey, D.P. (2000). Two mechanisms for transducer adaptation in vertebrate hair cells. Proc. Natl. Acad. Sci. USA *97*, 11730–11735.

Holt, J.R., Corey, D.P., and Eatock, R.A. (1997). Mechanoelectrical transduction and adaptation in hair cells of the mouse utricle, a low-frequency vestibular organ. J. Neurosci. *17*, 8739–8748.

Holt, J.R., Vollrath, M.A., and Eatock, R.A. (1999). Stimulus processing by type II hair cells in the mouse utricle. Ann. N Y Acad. Sci. *871*, 15–26.

Howard, J., and Hudspeth, A.J. (1987). Mechanical relaxation of the hair bundle mediates adaptation in mechanoelectrical transduction by the bullfrog's saccular hair cell. Proc. Natl. Acad. Sci. USA *84*, 3064–3068.

Howard, J., and Hudspeth, A.J. (1988). Compliance of the hair bundle associated with gating of mechanoelectrical transduction channels in the bullfrog's saccular hair cell. Neuron *1*, 189–199.

Kachar, B., Parakkal, M., Kurc, M., Zhao, Y., and Gillespie, P.G. (2000). High-resolution structure of hair-cell tip links. Proc. Natl. Acad. Sci. USA *97*, 13336–13341.

Kapoor, T.M., and Mitchison, T.J. (1999). Allele-specific activators and inhibitors for kinesin. Proc. Natl. Acad. Sci. USA *96*, 9106–9111.

Kros, C.J., Marcotti, W., van Netten, S.M., Self, T.J., Libby, R.T., Brown, S.D.M., Richardson, G.P., and Steel, K.P. (2002). Reduced climbing and increased slipping adaptation in cochlear hair cells of mice with mutations in the *Myo7a* gene. Nat. Neurosci. *5*, 41–47.

Pestic-Dragovich, L., Stojiljkovic, L., Philimonenko, A.A., Nowak, G., Ke, Y., Settlage, R.E., Shabanowitz, J., Hunt, D.F., Hozak, P., and de Lanerolle, P. (2000). A myosin I isoform in the nucleus. Science *290*, 337–341.

Pusch, M., and Neher, M. (1988). Rates of diffusional exchange between small cells and measuring patch pipette. Pflugers Arch. *411*, 204–211.

Ruppert, C., Godel, J., Muller, R.T., Kroschewski, R., Reinhard, J., and Bahler, M. (1995). Localization of the rat myosin I molecules myr 1 and myr 2 and in vivo targeting of their tail domains. J. Cell Sci. *108*, 3775–3786.

Rybin, V., Ullrich, O., Rubino, M., Alexandrov, K., Simon, I., Seabra, C., and Goody, R. (1996). GTPase activity of Rab5 acts as a timer for endocytic membrane fusion. Nature *383*, 266–269.

Shah, K., Liu, Y., Deirmengian, C., and Shokat, K.M. (1997). Engineering unnatural nucleotide specificity for Rous sarcoma virus tyrosine kinase to uniquely label its direct substrates. Proc. Natl. Acad. Sci. USA *94*, 3565–3570.

Shepherd, G.M.G., and Corey, D.P. (1994). The extent of adaptation in bullfrog saccular hair cells. J. Neurosci. *14*, 6217–6229.

Sherr, E.H., Joyce, M.P., and Greene, L.A. (1993). Mammalian myosin Iα, Iβ, and Iγ: new widely expressed genes of the myosin I family. J. Cell Biol. *120*, 1405–1416.

Shioda, T., Egi, Y., Yamada, K., and Kawasaki, T. (1991). Properties of thiamin triphosphate-synthesizing activity of chicken cytosolic adenylate kinase and the effect of adenine nucleotides. Biochim. Biophys. Acta *1115*, 30–35.

Steyger, P.S., Gillespie, P.G., and Baird, R.A. (1998). Myosin Iβ is located at tip link anchors in vestibular hair bundles. J. Neurosci. *18*, 4603–4615.

Walker, R.G., and Hudspeth, A.J. (1996). Calmodulin controls adaptation of mechanoelectrical transduction by hair cells of the bullfrog's sacculus. Proc. Natl. Acad. Sci. USA *93*, 2203–2207.

Wu, Y.C., Ricci, A.J., and Fettiplace, R. (1999). Two components of transducer adaptation in auditory hair cells. J. Neurophysiol. *82*, 2171–2181.

Yamoah, E.N., and Gillespie, P.G. (1996). Phosphate analogs block adaptation in hair cells by inhibiting adaptation-motor force production. Neuron *17*, 523–533.